

## Pseudotachylyte and the development of ultramylonite bands in the Saint-Barthélemy Massif, French Pyrenees

C. W. PASSCHIER\*

Geologisch Instituut, Nieuwe Prinsengracht 130, 1018 VZ Amsterdam, The Netherlands

(Received 6 August 1981; accepted in revised form 4 November 1981)

**Abstract**—In mylonitic gneisses of the Saint-Barthélemy Massif in the French Pyrenees, evidence was found that ultramylonite bands developed by ductile deformation of pseudotachylyte.

In the gneiss a mylonitic shape fabric was produced by a continuous structural event during retrogression from amphibolite to upper greenschist facies. Decrease in temperature caused gradual hardening in the gneiss which led to the development of pseudotachylyte bands by intermittent seismic slip. These acted as weak zones in which ductile deformation was concentrated. A microstructure typical of ultramylonite was produced in these deformed pseudotachylyte bands.

### INTRODUCTION

ULTRAMYLONITE and pseudotachylyte have many macro- and microstructural properties in common, but are often separated as being formed by different mechanisms.

Ultramylonite is thought to be the product of crystal plastic and subsidiary brittle deformation mechanisms in ductile shear zones. Pseudotachylyte is thought to develop by local melting of the rock due to heat generated during seismic slip along active brittle shear fractures. Both rock types can usually be distinguished by the following criteria.

Pseudotachylyte bands commonly display injection veins intruding the surrounding rock. Microstructurally they consist of a dark, occasionally glassy matrix. When crystalline, the matrix may contain microlites, spherulites and devitrification structures but lacks a mica preferred orientation. The matrix usually displays a sharp contact with the adjacent intact rock. Numerous relatively angular mineral and rock fragments lie in the matrix. They do not show evidence of stronger ductile deformation than that undergone by the surrounding rock. Chemical corrosion of minerals adjacent to the matrix, especially of biotite and hornblende, is common (e.g. Masch 1973, Park 1961).

In contrast, ultramylonite bands lack injection veins. The matrix is never glassy and does not contain microlites and spherulites. A compositional layering and a preferred orientation of micas in the matrix is common. The contact with the adjacent rocks is gradational. Flattened, commonly recrystallized mineral aggregates and porphyroclasts lie parallel to the compositional layering (e.g. Bell & Etheridge 1973, Kerrich *et al.* 1980).

It is usually suggested that ultramylonite develops by progressive mylonitisation at deeper crustal levels where ductile deformation is dominant, and pseudotachylyte at shallower levels (Sibson 1975, 1977, White *et al.* 1980).

Sibson (1977, 1980) envisaged a transitional regime in which mylonitisation and pseudotachylyte formation overlapped, and demonstrated that in some circumstances ultramylonite bands may result from the deformation of pseudotachylyte vein complexes. In gneiss of the Saint-Barthélemy Massif, evidence was found that ultramylonite bands can develop from pseudotachylyte in this transitional regime.

### REGIONAL SETTING

The Saint-Barthélemy Massif is one of the Northern Pyrenean massifs in France (Fig. 1). It consists of a gneiss core which is covered by sediments of Palaeozoic age. The gneiss core can be subdivided into a basal unit probably of Precambrian age, covered by migmatitic gneisses of Hercynian age (Guchereau 1975, Zwart 1954, 1979).

A main structural event caused intense deformation in the gneiss. The result is a well developed shape fabric in the Basal Gneiss Unit and in the lower part of the migmatitic gneiss, called the Lower Gneiss Unit. The upper part, called the Upper Gneiss Unit, does not contain deformation fabrics.

The shape fabric in the Lower Gneiss Unit is best developed in a 3–20 m thick Main Mylonite Band which forms the boundary with the Upper Gneiss Unit (Fig. 1). The orientation of the planar and linear elements of the shape fabric,  $S_g$  and  $L_g$ , is illustrated in Fig. 2.

The Lower Gneiss Unit was studied in detail. It consists mainly of homogeneous granitic gneiss. Mineral parageneses are typical of the amphibolite facies, containing quartz, oligoclase, orthoclase, biotite, muscovite, sillimanite, almandine, cordierite and zircon. The main structural event postdates the peak of metamorphism and continued during the following retrogression to lower greenschist facies conditions. This can be demonstrated by different subsequent parageneses of deformed mineral grains. Deformation in the gneiss was mainly by ductile deformation and recrystallization of quartz, biotite and

\* Present address: Department of Geology, University College, Swansea SA2 8PP, Wales, U.K.

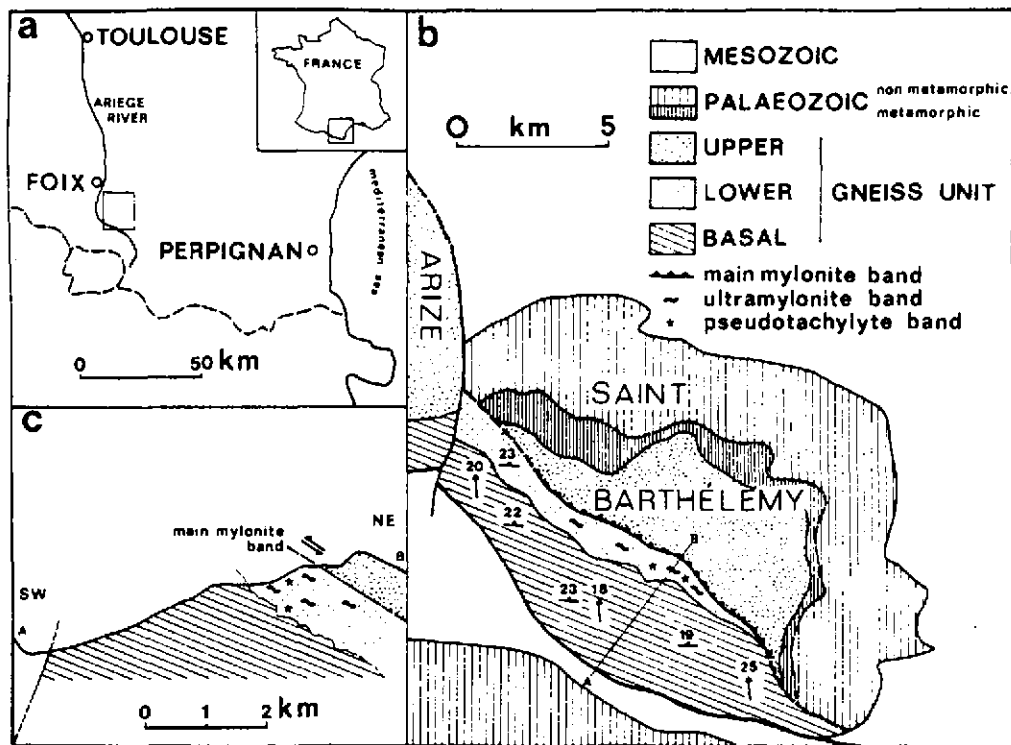


Fig. 1. (a) Position of the area in France. (b) Simplified map of the Saint-Barthélemy Massif based on the maps of Zwart (1979). The localities where ultramylonite bands and pseudotachylyte bands occur are indicated. (c) Schematic cross section through the gneiss core of the massif showing the orientation of the contacts between the different units.

muscovite and by brittle and ductile deformation of feldspar.

In the Lower Gneiss Unit a large number of isolated dark bands can be observed, usually cross-cutting  $S_0$  at a gentle angle and invariably dipping less steeply to the north than  $S_0$  in outcrop (Fig. 3). Based on microstructural and field criteria, two types of bands could be distinguished: ultramylonite and pseudotachylyte bands.

#### ANALYTICAL TECHNIQUE

The structure of dark bands (both pseudotachylyte and ultramylonite) and their geometrical relationship with the shape fabric in the gneiss were studied in detail in the field. The appearance of the bands strongly depends on the orientation of the outcrop surface (Fig. 3). This orientation was carefully noted and the data from surfaces with identical orientation were used to construct a three dimensional model of the bands. Nearly 200 dark bands were described and measured in the field. Their microstructure has been studied in over a hundred oriented thin sections.

The fine-grained matrix of dark bands has been investigated by electron microscopy. Discs of material 1 cm in diameter were polished and mounted on aluminium specimen tables. The polished surface was etched in vapour of 40% HF at 25°C. Usually, exposure at 1 cm over the HF basin for 2–10 seconds was sufficient to make the microstructure visible by scanning electron microscope (SEM). The mineral composition of the matrix and porphyroclasts was detected in carbon covered

specimens observed in a STEREOSCAN S 150-SEM with energy dispersive X-ray analysis (EDAX) using a LINK system type 290. The microstructure of the matrix was studied on Au–Pd covered specimens in a CAMBRIDGE M2A-SEM. The different minerals which were previously detected by EDAX on carbon covered specimens, could be recognized due to their different brightness and response to etching. The sequence biotite–feldspar–white mica–quartz has increasing resistance to etching and the sequence plagioclase–alkali feldspar–quartz–white mica–biotite has increasing brightness. Boundaries between individual quartz grains could not be etched with the method used. This is the reason why quartz appears as a continuous field in the SEM photographs.

Dislocation density in different mineral grains of the matrix was analysed with a JEOL 200C-STEM coupled to the same LINK system. This made determination of individual mineral grains possible.

#### ULTRAMYLONITE BANDS

##### *Field aspects*

In outcrop, ultramylonite bands are isolated dark bands with a homogeneous aphanitic appearance and sharp straight boundaries separating them from the surrounding gneiss (Fig. 4). In three dimensions they are planar disc-shaped bodies, 1–5 mm thick and 5–50 m in diameter. The bands usually cut through the surrounding gneiss without important branching or abrupt changes in

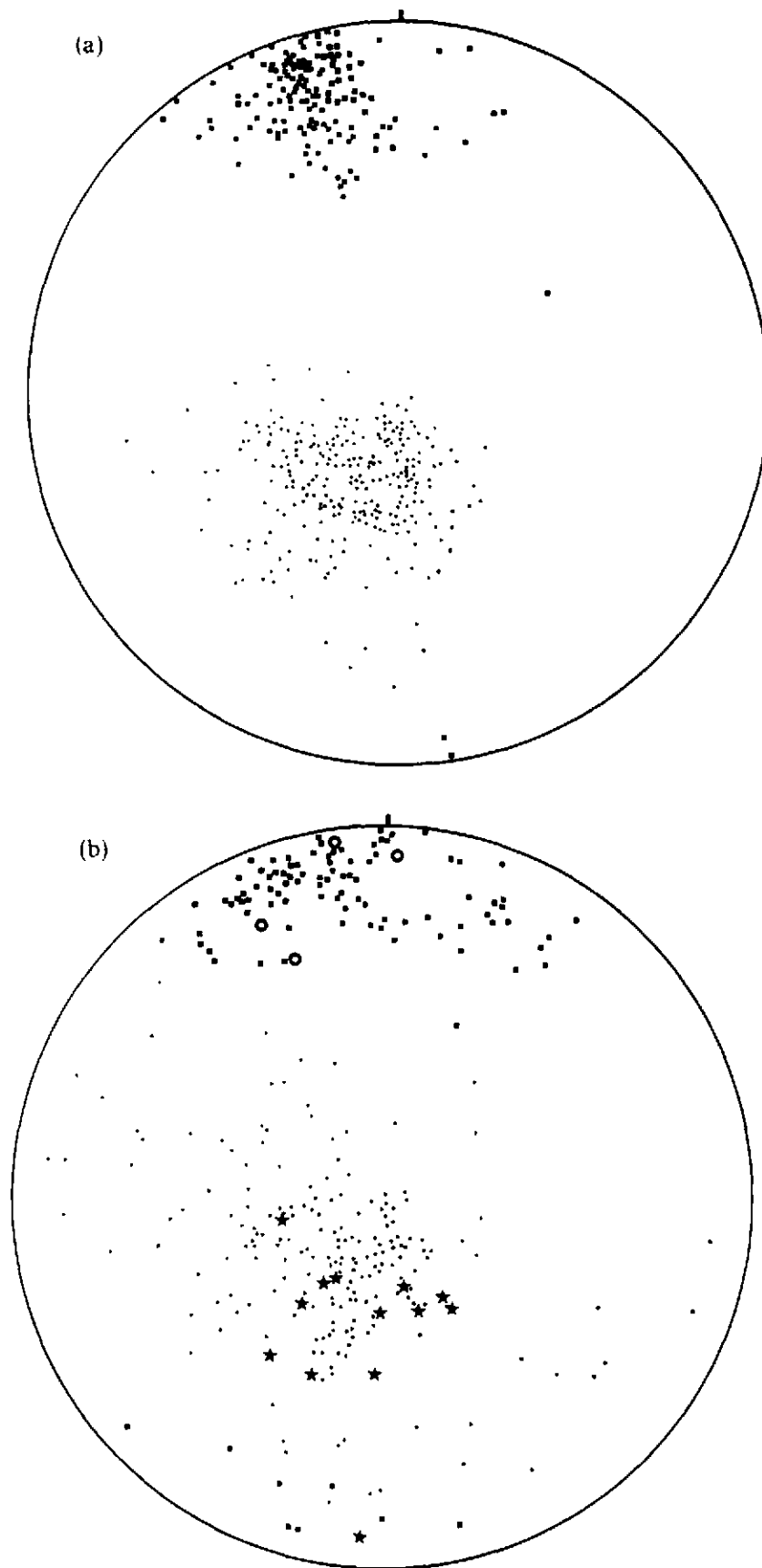


Fig. 2. (a) Stereogram showing the orientation of the shape fabric in the Lower Gneiss Unit; dots indicate poles to the planar elements ( $S_g$ -262 points) and squares indicate the linear elements ( $L_g$ -143 points). (b) Stereogram showing the orientation of ultramylonite bands (dots-192 poles), the stretching lineation  $L_u$  in them (squares-111 points), the available data on the orientation of pseudotachylite main bands (stars-poles) and the stretching lineation  $L_p$  in them (open circles). Equal area projections, lower hemisphere.

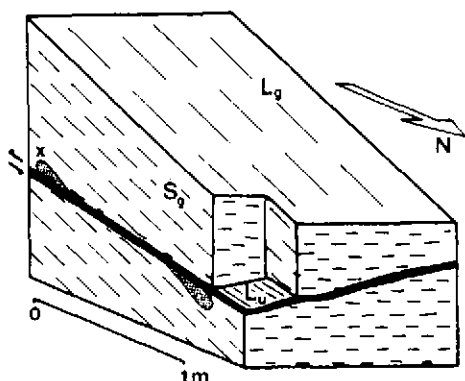


Fig. 3. Schematic representation of the typical spatial relationship of an ultramylonite band (black) and the shape fabric in the gneiss.  $S_g$  and  $L_g$  are the planar and linear elements of the shape fabric in the gneiss.  $L_u$  is the stretching lineation in the ultramylonite band.  $S_u$  is deflected near the band and a xenolith (X) is cut and displaced. The direction of displacement typical for ultramylonite bands is marked.

thickness (Fig. 3). They terminate by branching and tapering of the bands over a distance up to a metre. In all cases these branches tend to run subparallel to  $S_g$ , whatever the orientation of the band. This implies that a band making an angle with  $S_g$  changes its orientation into approximate parallelism near its termination. An internal stretching lineation defined by rod-shaped aggregates of recrystallized quartz, feldspar and biotite is usually present in the bands ( $L_u$ ). Its orientation is almost identical to that of  $L_g$  in outcrop, but  $L_u$  tends to plunge less steeply to the north (Fig. 2). On outcrop surfaces parallel to  $L_g$  one can often observe that  $S_g$  is deflected by the band (Fig. 3). Xenoliths are cut and displaced along the bands in a direction subparallel to  $L_u$ , consistently in such a way that the upper block moved relatively to the south (Fig. 3).

Shear strains reached in the bands are rather high. Displacement of xenolith fragments along a 1 mm thick band of up to 1 m occurs. Recrystallized aggregates of apatite in the bands are extremely flattened. Their shape indicates that shear strains up to 1800 are locally reached, assuming the aggregates originated from equidimensional coarse apatite grains which occur in the surrounding gneiss.

#### Microstructure

The microstructure of ultramylonite bands is fairly regular. It consists of a homogeneous dark fine-grained matrix of quartz, albite-oligoclase and biotite with a few isolated porphyroclasts of quartz, feldspar, sillimanite, zircon and almandine together with lenses of dynamically recrystallized quartz, feldspar and apatite. The boundary with the surrounding gneiss is sharp in the field but a gradual transition, over 0.1–1 mm, was observed in thin section. The grain size in the matrix is 1–5  $\mu\text{m}$ , an observation which explains the aphanitic appearance in outcrop. A weak compositional layering defined by alternating biotite and quartz-feldspar rich lenses is developed subparallel to the margins of the band (Fig. 5). Biotite in the matrix has an extremely strong preferred orientation which makes a small angle with the compositional layering with a sense as indicated in Fig. 5. This

results in uniform pleochroism and extinction in the band when the microscope stage is turned (Fig. 5).

The preferred orientation of single biotite grains can be observed by SEM (Fig. 6a): most grains have the same orientation except where they are deflected around porphyroclasts.

## PSEUDOTACHYLYTE BANDS

Ten per cent of the investigated dark bands exhibit the criteria typical of a pseudotachylyte. Their orientation is similar to that of ultramylonite bands, usually cutting through  $S_g$  and rarely parallel to it (Figs. 2 and 3). The pseudotachylyte bands show narrow, irregular, branching injection veins intruding at a high angle from the main band into the surrounding gneiss (Francis 1972, Sibson 1975). No significant displacement across these injection veins could be observed (Fig. 7). Both undeformed and deformed pseudotachylyte bands have been found.

#### Undeformed pseudotachylyte—microstructure

The microstructure of undeformed bands consists of a dark matrix with many xenocrysts of quartz, feldspar, zircon, sillimanite and almandine together with included gneiss fragments. The bands are separated from the surrounding gneiss by a sharp contact on a microscopic scale, in contrast with the transition zone of ultramylonite bands (Fig. 8a). Grain and subgrain boundaries in quartz grains along the contact are cut off and therefore formed prior to the formation of the pseudotachylyte bands (Fig. 8a).

The matrix consists of albite-oligoclase, quartz, biotite and occasionally white mica. Biotite lacks a preferred orientation as illustrated by observations with SEM (Fig. 6b). Many xenocrysts are armoured by radially arranged microlites of biotite and feldspar (Fig. 8b). Spherulites occur around xenocrysts as layered coronas of alternating mineral composition. Interference of these coronas may cause the 'cauliflower head' structure visible in thin section (Fig. 8c).

Xenocrysts of quartz with an irregular shape are common. They usually have a sharp contact with the matrix (Fig. 8d). Fine, dispersed ore particles and fractures bordered by solid and fluid inclusions are typically present in quartz xenocrysts (Fig. 8e). Irregularly shaped aggregates of fine-grained plagioclase or alkali feldspar occur locally.

Quartz and feldspar grains of the country rock along the contact of the bands are cut by numerous healed fractures and often by micro injection veins (Fig. 8a). Biotite grains up to 10 cm away from the bands display repeated narrow kinks uncommon elsewhere in the gneiss.

#### Deformed pseudotachylyte—microstructure

More than fifty per cent of the investigated pseudotachylyte bands were affected by ductile deformation

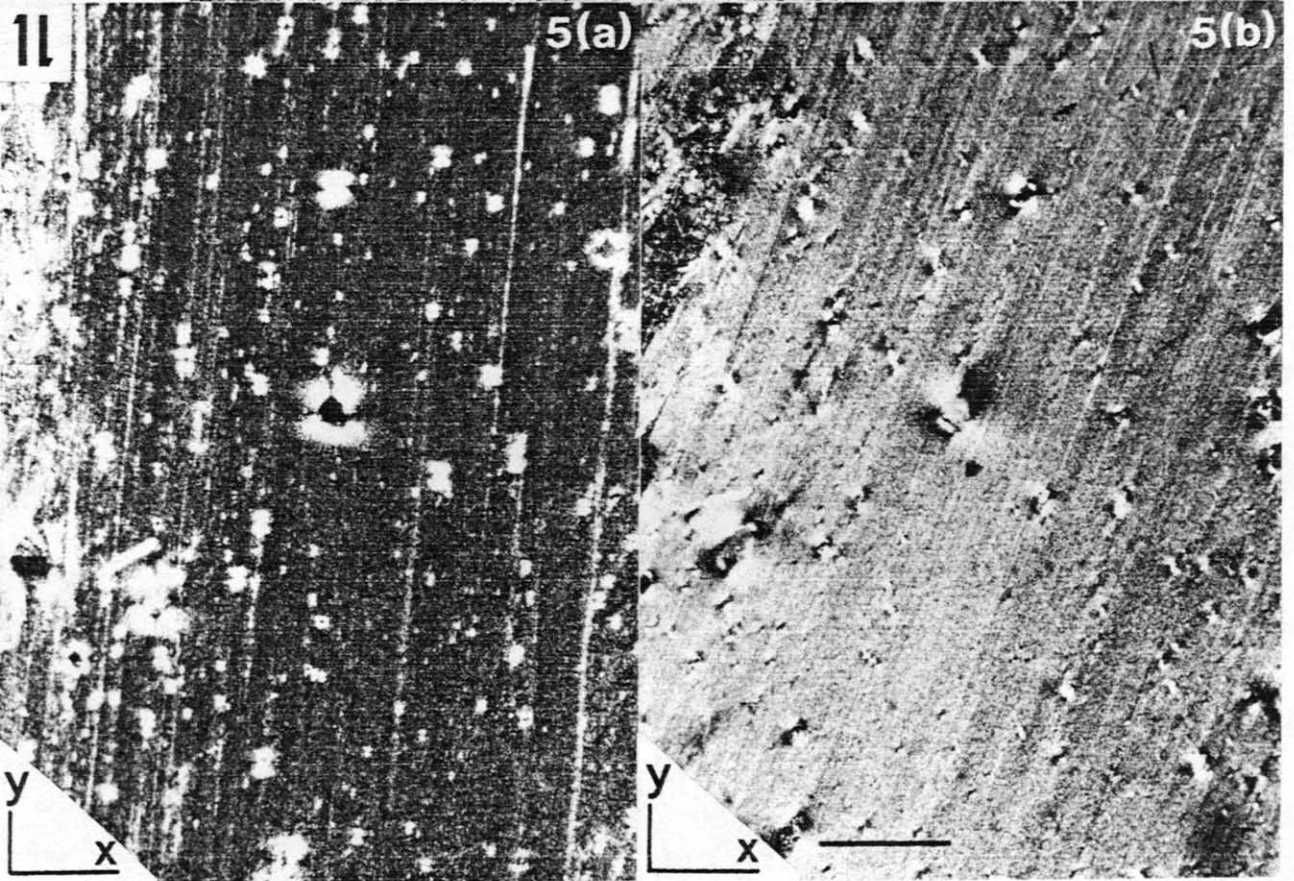
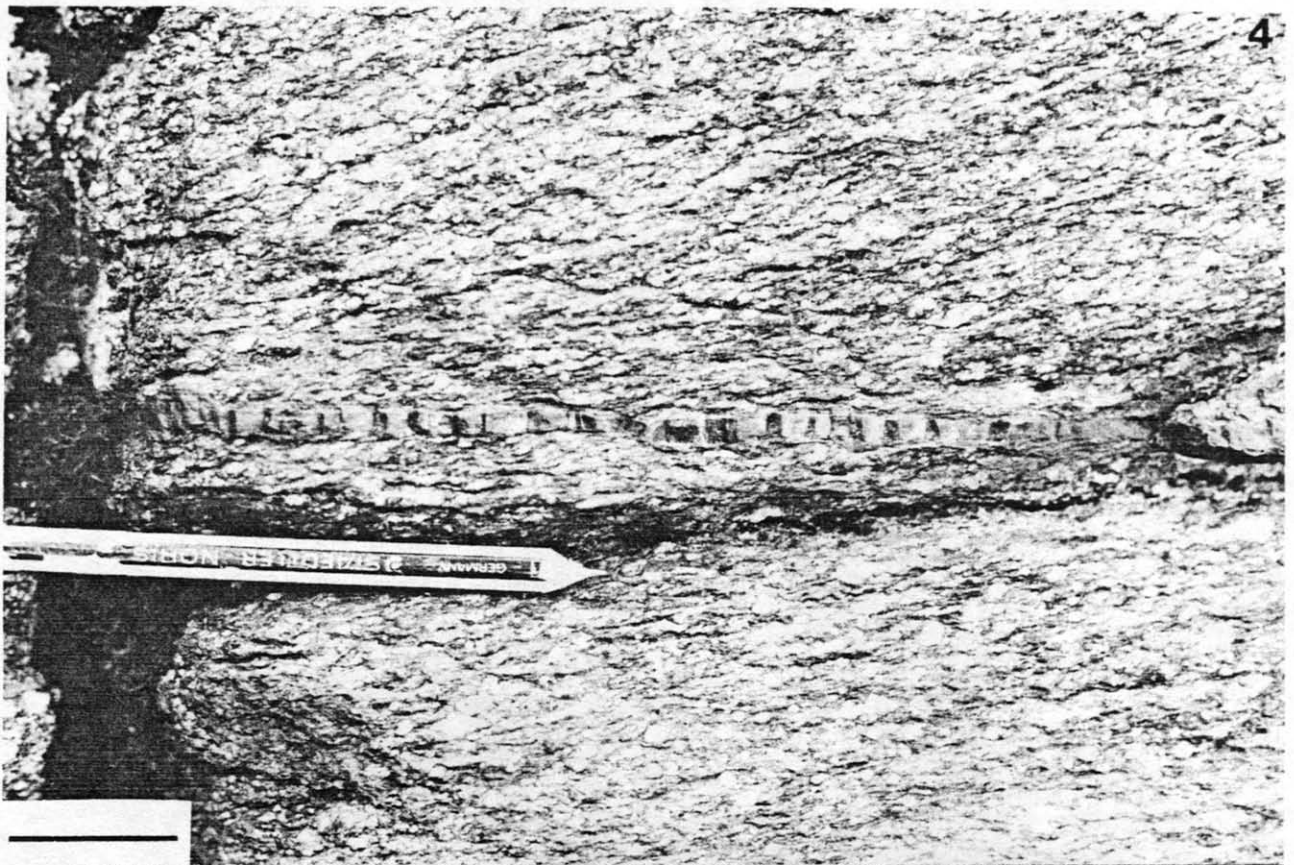


Fig. 4. Field aspect of a typical ultramylonite band. The boundary with the gneiss is sharp, and the band makes an angle with the foliation in the gneiss. Scale bar 3 cm.

Fig. 5. Microstructure of an ultramylonite band on a section parallel to  $L_p$ . Crossed polars shown by lines  $x$  and  $y$ . (a) Compositional layering nearly vertical. The matrix is dark due to uniform extinction of biotite grains which have a strong preferred orientation. Bright lobes round inclusions are caused by deflection of the biotite preferred orientation around them; (b) Same picture, but rotated  $20^\circ$ , which rotates most micas out of the extinction position. Some lobes around the inclusions are darker or brighter than the bulk matrix through their deviant orientation. Scale bar 0.5 mm.



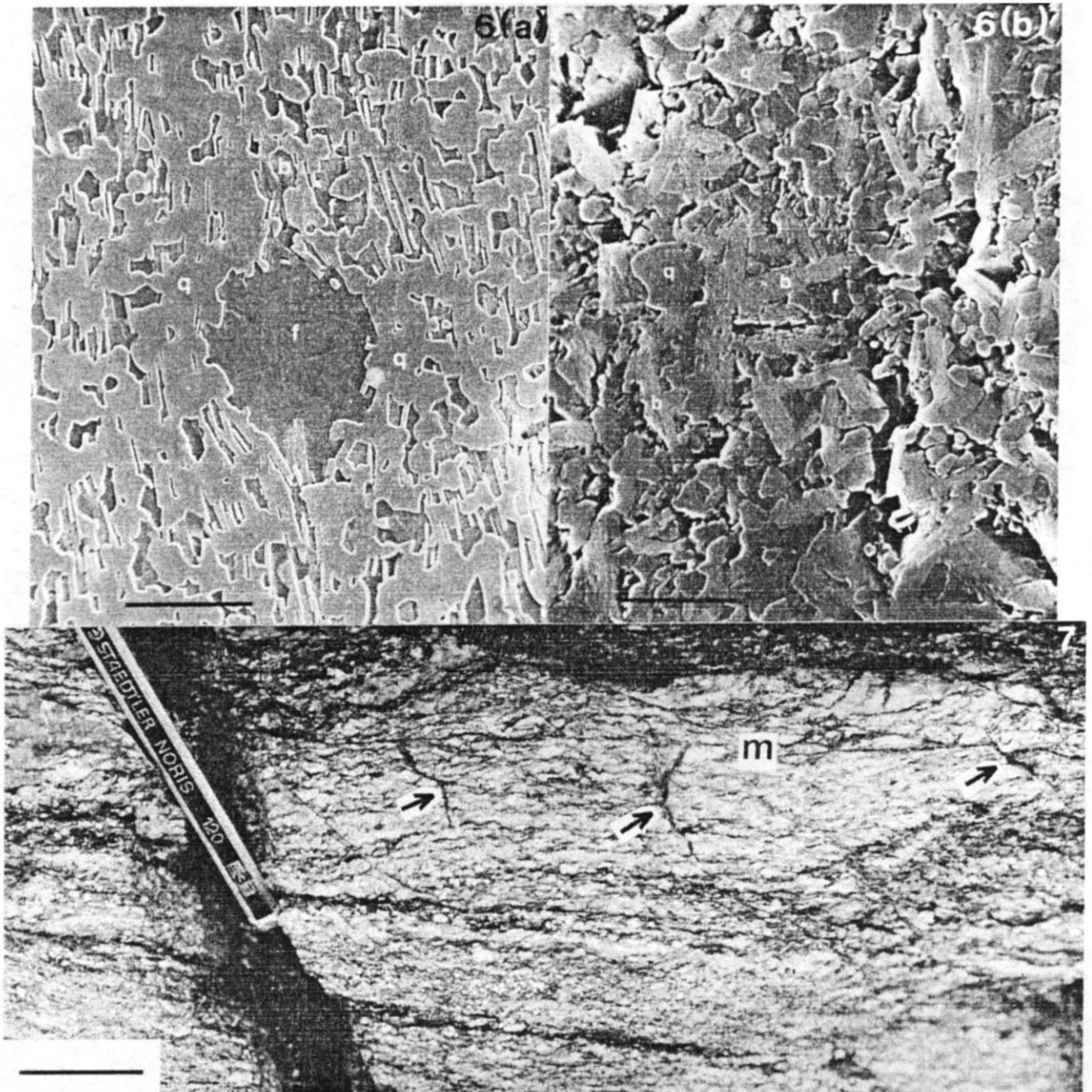


Fig. 6. Microstructure of the matrix of dark bands as observed by SEM on polished and etched specimens, Au-Pd covered : q, quartz; f, feldspar; b, biotite. (a) Ultramylonite, a well developed biotite preferred orientation curves round a feldspar porphyroclast (scale bar 10  $\mu\text{m}$ ). (b) Undeformed pseudotachylyte, biotite has a random orientation (scale bar 5  $\mu\text{m}$ ).

Fig. 7. Field aspect of a pseudotachylyte band. Small injection veins (arrows) leave the main band (m). Scale bar 3 cm.

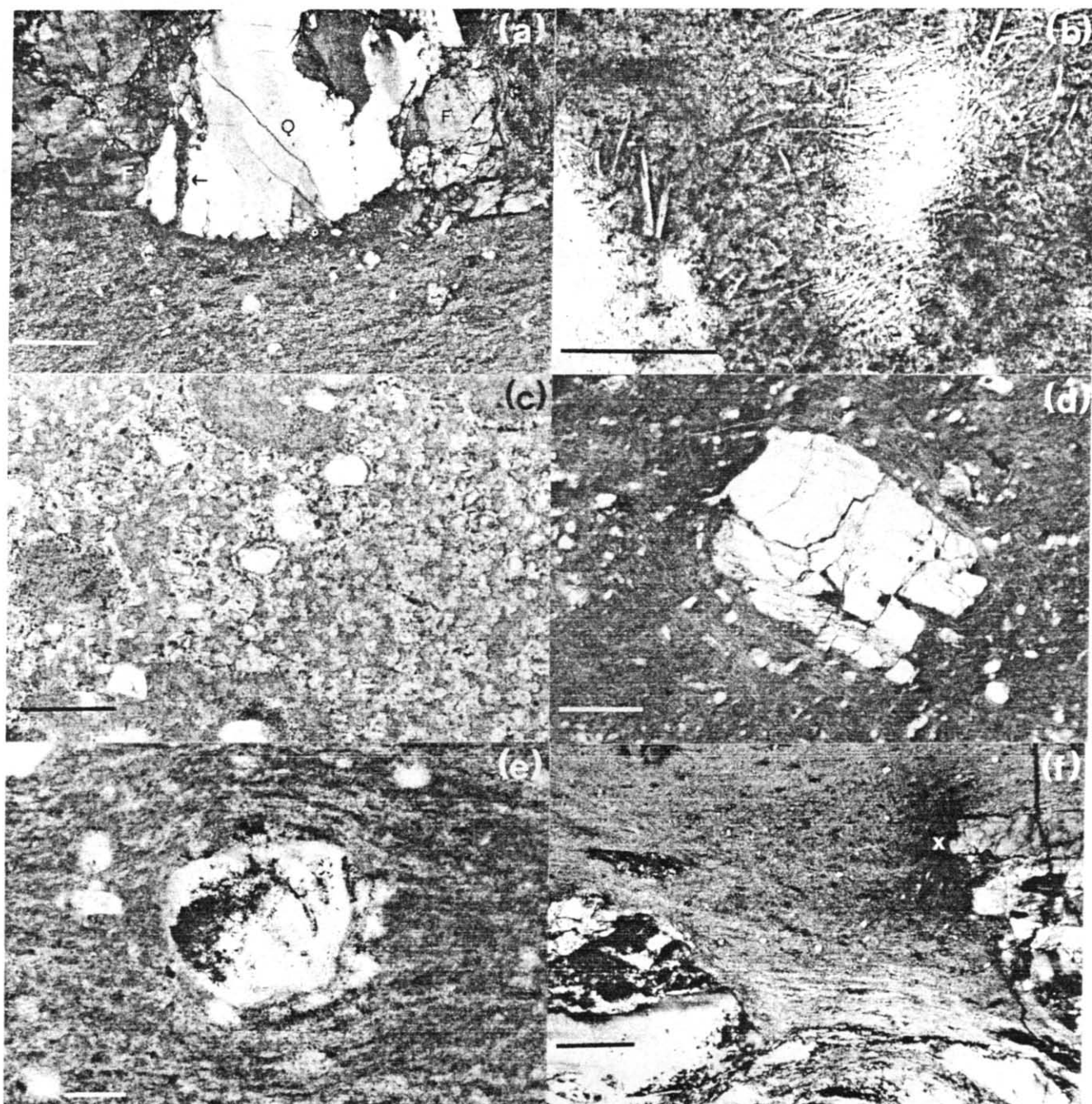
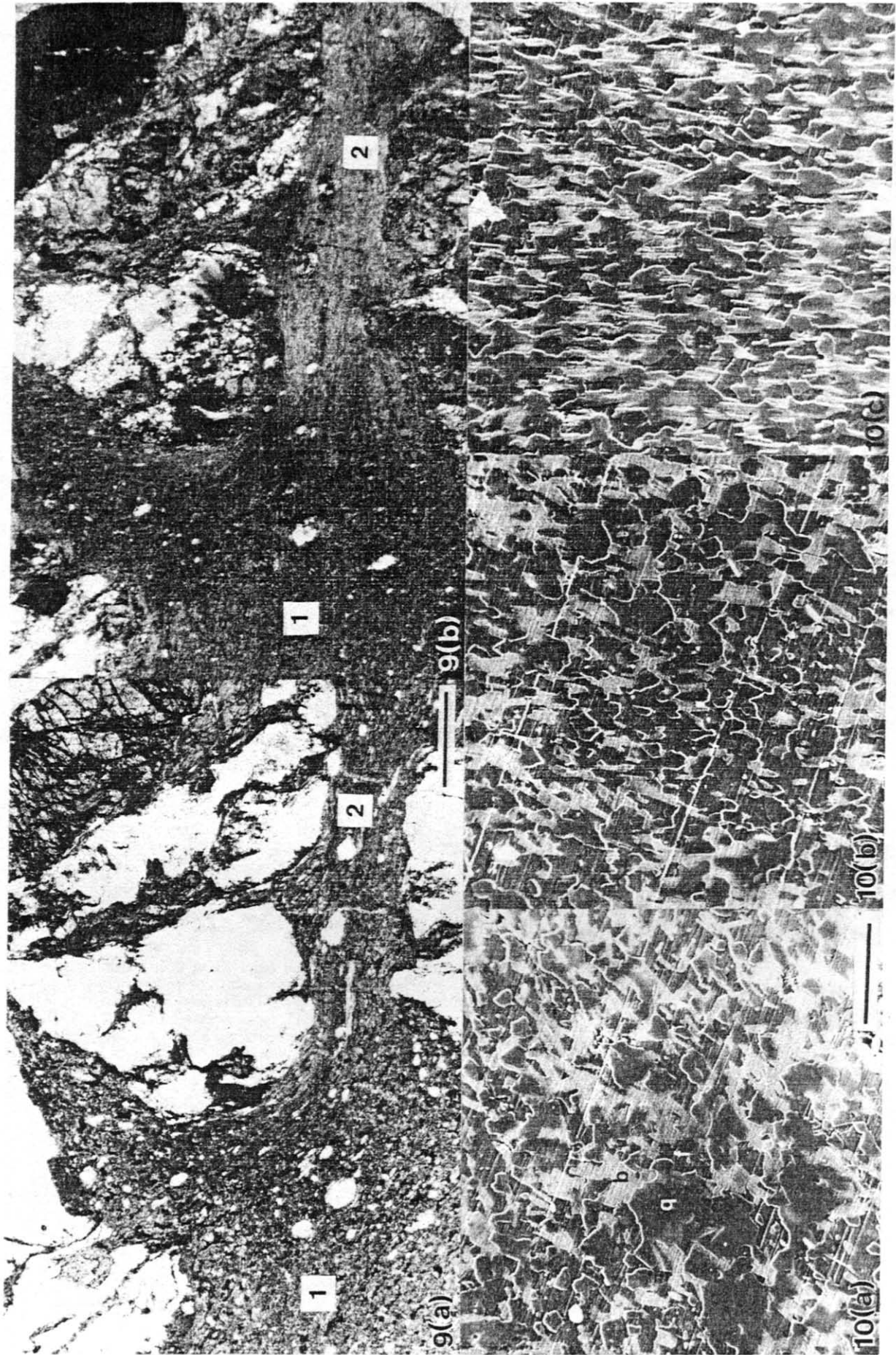


Fig. 8. (a) Margin of a pseudotachylyte band. The contact between the fine grained matrix and quartz (Q) and alkali feldspar (F) grains in the surrounding gneiss is sharp. Subgrain boundaries in quartz are cut by the contact. A micro-injection vein runs into the quartz grain (arrow), scale bar 0.5 mm. (b) Feldspar microclites in the matrix of an undeformed pseudotachylyte band, radially arranged round a quartz inclusion, scale bar 0.1 mm. (c) Spherulites in the matrix of an undeformed pseudotachylyte band, arranged in radial pattern round inclusions, scale bar 0.5 mm. (d) Quartz xenocryst in the matrix of an undeformed pseudotachylyte band with angular shape and sharp boundaries. Healed fractures lined with fluid inclusions cut the xenocryst, scale bar 0.5 mm. (e) Fine, dispersed ore grains in a quartz xenocryst in the matrix of a weakly deformed pseudotachylyte band. A weak layering starts to develop and curves around the xenocryst, scale bar 0.1 mm. (f) Contact of a strongly deformed pseudotachylyte band with the surrounding gneiss. The contact is sharp, irregular and forms an embayment in the gneiss. A biotite preferred orientation is developed in the matrix except in part of the embayment (X), scale bar 0.5 mm.





(Passchier 1981). In the field they exhibit a stretching lineation with an orientation analogous to that in ultramylonite bands (Fig. 2). Injection veins have been flattened, rotated parallel to  $S_p$  and are mesoscopically hard to distinguish from lenticular biotite aggregates in the gneiss.

In thin section the characteristic spherulitic structures are flattened. Xenocrysts of quartz and feldspar are ductilely-deformed, often dynamically recrystallized and have acquired a lenticular shape. In the matrix a weak biotite preferred orientation is developed ( $S_p$ ). In some injection veins with irregular shape, a gradual transition can be observed from undeformed to deformed parts (Fig. 9). Observations by SEM of the matrix of such a specimen show the gradual development of a biotite preferred orientation without changes in grain size, grain shape or mineral composition (Fig. 10). In the case illustrated the transition takes place over 5 mm.

In strongly deformed pseudotachylyte bands the entire centre of the band has a well developed  $S_p$ , nearly as strong as the biotite preferred orientation in ultramylonite bands. Small embayments of pseudotachylyte matrix along the irregular contact with the gneiss may lack this foliation (Fig. 8f). The transition to the centre of the band, where  $S_p$  is well developed, is gradual.

### METAMORPHIC CONDITIONS

Deformation in the ultramylonite and pseudotachylyte bands took place under upper greenschist facies conditions. Sillimanite xenocrysts in the bands were unstable; they occur as relics, locally transformed to muscovite. Almandine with a high spessartine content, biotite, muscovite and albite formed a stable paragenesis. Chlorite and epidote are not present.

### DISCUSSION

Ultramylonite bands can be classified as narrow ductile shear zones with sharp boundaries. Both the mesoscopic and microscopic structure of the bands are comparable with those of ultramylonites described by Bell & Etheridge (1973) and Kerrich *et al.* (1980). The microstructures observed are indicative of ductile deformation mechanisms and minor brittle deformation of some porphyroclasts. Deflection of  $S_p$  and displacement of xenoliths by the bands in sections parallel to  $L_u$  indicates a consistent lateral displacement direction along them.

The pseudotachylyte bands observed are similar to those described from other areas, both in the presence of injection veins and in their microstructure (e.g. Ermanovics *et al.* 1972, Francis & Sibson 1973, Masch 1973,

1979, Park 1961, Sibson 1975). These bands developed by local melting of the rock in response to frictional heat generated by seismic slip on a brittle shear fracture (e.g. Allen 1979, Francis 1972, Sibson 1975, 1977, Watts & Williams 1979).

In deformed pseudotachylyte bands, the characteristic meso- and microstructure was partly obliterated and overprinted by structures formed during ductile deformation, in particular by the development of a biotite preferred orientation ( $S_p$ ). This structure is produced by ductile deformation in pseudotachylyte and is not due to mimetic control exercised by a flow fabric in the pseudotachylyte because:

(a) where a primitive banding due to compositional difference exists, it has domains which are obliquely cut by  $S_p$  in an unsystematic way;

(b)  $S_p$  is often subparallel to the walls of the pseudotachylyte bands and gradually decreases in intensity into injection veins, remaining in nearly the same orientation; this causes  $S_p$  to be oblique to the walls of the injection vein, which is hard to explain as a feature inherited from a flow fabric and

(c) in injection veins,  $S_p$  is often developed only in the narrow tips of the veins which are most sensitive to flattening of the vein but not supposed to have the strongest flow fabric; from the narrow tip  $S_p$  fans out into the wider part of the vein and often disappears.

Several observations indicate that diffusion-accommodated grain-boundary sliding, possibly in a superplastic regime, was the most important deformation mechanism in the matrix of deformed pseudotachylyte and ultramylonite bands. This conclusion is based on criteria postulated by Boullier & Gueguen (1975), Edington *et al.* (1976) and Schmid *et al.* (1977). No change in grain size, grain shape or mineral composition took place during progressive deformation of the matrix of a pseudotachylyte band. The matrix of the dark bands is polymineralic, the grain size is small and dislocation densities in the grains are low as observed by STEM.

Strongly-deformed pseudotachylyte bands are dominated by microstructural features which were described above as being characteristic of ultramylonite bands. The different types of band can only be distinguished if relics of the pseudotachylyte microstructure are present. Such relics are deformed spherulites, finely-dispersed ore in quartz grains, angular quartz xenocrysts, injection veins and embayments which lack development of  $S_p$ . Since all gradations exist between undeformed pseudotachylyte and ultramylonite it may be inferred that at least some of the ultramylonite bands are in fact ductilely-deformed pseudotachylyte veins. It is very likely, however, that many of the ultramylonite bands developed directly from

Fig. 9. Microstructure of a partly deformed pseudotachylyte injection vein. (a) Uncrossed polars. In the widest part of the vein (1) quartz xenocrysts and spherulitic structures (black) are hardly deformed and equidimensional. In the narrow part (2) the matrix is strongly deformed and both have a lens shape. (b) Crossed polars. At (2) a strong biotite preferred orientation is developed decreasing in strength towards (1). Scale bar 0.5 mm.

Fig. 10. SEM photographs of the matrix of a partly deformed pseudotachylyte main band. q, quartz; f, feldspar; b, biotite. The pictures are taken in sequence over 5 mm from undeformed (a), moderately deformed (b), to strongly deformed (c). A biotite preferred orientation is clearly developed from (a) to (c), while no change in mineral composition can be seen. Striping from upper left to lower right is due to polishing. Scale bar 10  $\mu$ m.

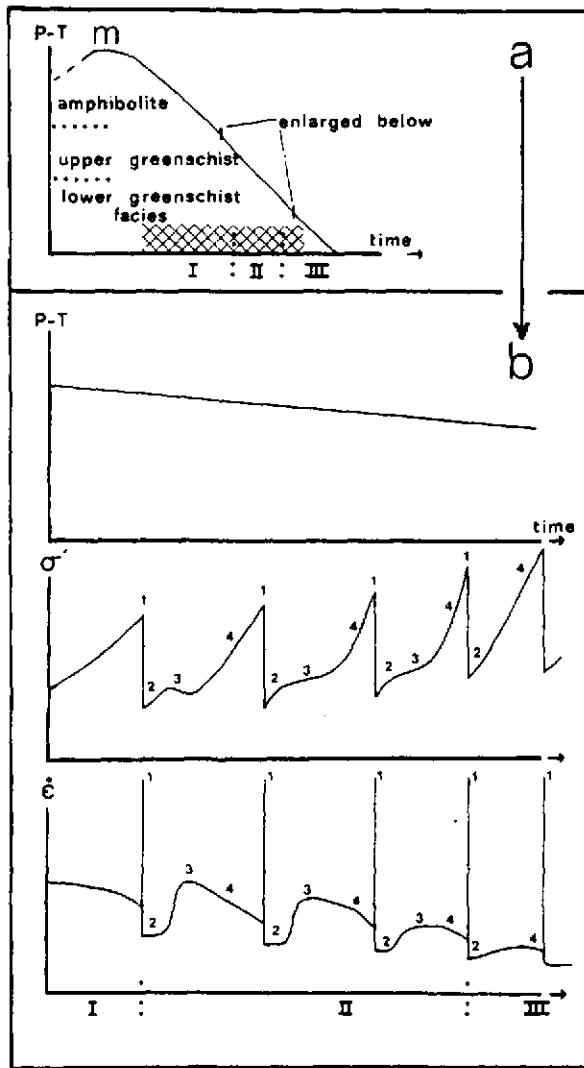


Fig. 11. Diagram of changes of external variables with time in a small volume of gneiss from the Lower Gneiss Unit during the main structural event. (a) Changes in mean stress ( $P$ ) and temperature ( $T$ ) with time. I, II and III are fields of dominantly ductile, ductile and brittle deformation respectively. The crosshatched area indicates the timespan of the main structural event.  $M$  = peak of Hercynian metamorphism. (b) Detail of the timespan in which pseudotachylyte is generated.  $\sigma'$  = differential stress;  $\dot{\epsilon}$  = strain rate in the gneiss. The sequence of events as envisaged is; (1) brittle fracturing, generation of pseudotachylyte; (2) devitrification; (3) ductile deformation of pseudotachylyte, the bands acting as weak zones and (4) strain hardening in the deformed band until stage (1) is reached again when failure occurs elsewhere in the gneiss. During period III the existing pseudotachylyte does not act as a weak zone and deformation becomes dominantly brittle. The effects of ultramylonite bands which nucleated by grain size reduction are omitted for clarity.

the mylonitic gneiss by local grain size reduction. For most of the ultramylonite bands it cannot be decided if a pseudotachylyte stage was part of their formation history.

The development of a shape fabric in the gneiss and the formation of pseudotachylyte and ultramylonite bands all took place during the main structural event of progressive reverse shear: the orientations of the bands and their internal lineations are similar to the orientation of  $S_g$  and  $L_g$  (Fig. 2) and the mineral parageneses of the bands are consistent with the postulated retrogression during the main structural event.

The fact that pseudotachylyte was generated at a

crustal level where its subsequent ductile deformation was possible, may be related to the fact that all fluid inclusions observed in rocks from the Lower Gneiss Unit contain pure  $\text{CO}_2$ . As a result, the strain hardening during retrogression may have been higher than usual at similar crustal levels due to a lack of hydrolytic weakening, permitting pseudotachylyte generation.

The sequence of events envisaged in the Lower Gneiss Unit is shown in Fig. 11. During retrogression from amphibolite to upper greenschist facies conditions, a shape fabric was developed by dominantly ductile deformation in the gneiss. Decrease in temperature during retrogression was the main reason for gradual strain hardening leading to increasing differential stresses, and finally to the generation of pseudotachylyte. The pseudotachylyte bands acted as weak zones along which deformation was concentrated. This caused the transformation of pseudotachylyte into ultramylonite. The relative weakness of pseudotachylyte bands is well illustrated by the large strains in these zones and by the presence of undeformed matrix in embayments protected from deformation by the surrounding gneiss. This may be explained by the fact that the matrix was well suited for diffusion-accommodated grain boundary sliding due to its small grain size and polymineralic habit. This allowed ductile deformation at a much lower differential stress than that required for renewed brittle failure. Ductile deformation may have followed almost immediately after the brittle displacement.

Finally, deformation in the band stopped. This was probably caused by strain hardening in that part of the surrounding gneiss in which strain accommodation for displacement along the band occurred. This led to a renewed increase in differential stress and to the creation of new pseudotachylyte bands after which the process was repeated. After several of these cycles, the gradually falling temperature inhibited ductile deformation of the pseudotachylyte bands. Presumably this was due to increased strength of the gneiss, which made strain accommodation around a ductile-deforming pseudotachylyte band difficult. Hereafter only undeformed pseudotachylyte bands developed.

Ultramylonite bands which developed by local grain size reduction probably nucleated as a response to the cyclic increase in differential stress. Because of their small grain size, they acted as weak zones in accordance with the behaviour of pseudotachylyte bands. The gradually falling temperature probably inhibited their formation when pseudotachylyte generation was still possible.

A sequence of deformation events in which mylonite development is followed by the generation of pseudotachylyte is also common in other areas (e.g. Allen 1979, Ermanovics *et al.* 1972, Sibson 1977). Grocott (1977) explained this as being the result of gradual uplift and erosion of an active shear zone: mylonites formed in such a zone will be brought to higher crustal levels and may become cut by younger pseudotachylyte bands. Gradual uplift of the gneiss core of the Saint-Barthélemy Massif during the main structural event may explain the observed sequence of events in a similar way.

Deformed pseudotachylyte has only rarely been reported from other areas (Allen 1979, Sibson 1980, Watts & Williams 1979). This may be due to difficulties in its recognition, or to the non-continuous activity of most shear zones. Only when a shear zone has been continuously active during uplift will it demonstrate the subsequent products of its deformation history in the rock. In most cases however shear zones were intermittently active, and deformed pseudotachylyte bands will be found only where the present level of erosion coincides with the crustal level at which they were formed during one of the active periods of the shear zone. This is probably also the case in the Saint-Barthélemy Massif.

### CONCLUSIONS

The following conclusions can be drawn.

(1) A mylonitic shape fabric in the gneiss was cut by younger pseudotachylyte and ultramylonite bands during a deformation event which coincided with retrogression from amphibolite to lower greenschist facies conditions.

(2) Many pseudotachylyte bands were ductilely-deformed and developed fabrics similar to those of ultramylonite. At least some of the ultramylonite bands in the area formed in this way, while others may have developed by the usual process of grain size reduction.

(3) Crystallized pseudotachylyte and ultramylonite bands acted as weak zones in the gneiss along which ductile deformation was concentrated.

(4) The fine-grained polymineralic matrix of crystallized pseudotachylyte was well suited for diffusion-accommodated grain-boundary sliding as a dominant deformation mechanism and probably caused the weakness of the bands.

(5) Deformed pseudotachylyte bands are formed at crustal levels in between the zone where ductile deformation is dominant and the zone where brittle fracturing produces undeformed pseudotachylyte.

*Acknowledgements*—I thank J. Grocott, H. van Roermund, G. Lister, R. Lisle, C. Biermann and H. Stel for critically reading the manuscript and offering valuable suggestions.

### REFERENCES

- Allen, A. R. 1979. Mechanism of frictional fusion in fault zones. *J. Struct. Geol.* 1, 231–243.
- Bell, T. H. & Etheridge, M. A. 1973. Microstructure of mylonites and their descriptive terminology. *Lithos* 6, 337–348.
- Boullier, A. M. & Gueguen, Y. 1975. SP-Mylonites: Origin of some mylonites by superplastic flow. *Contr. Miner. Petrol.* 50, 93–104.
- Edington, J. W., Melton, K. N. & Cutler, C. P. 1976. Superplasticity. *Progr. Mater. Sci.* 1, 61–158.
- Ermanovics, I. F., Helmstaedt, H. & Plant, A. G. 1972. An occurrence of Archean pseudotachylyte from southeastern Manitoba. *Can. J. Earth Sci.* 9, 257–265.
- Francis, P. W. 1972. The pseudotachylyte problem. *Comments Earth Sci. Geophys.* 3, 35–53.
- Francis, P. W. & Sibson, R. H. 1973. The Outer Hebrides Thrust. In: *The early Precambrian of Scotland and Related rocks of Greenland*. (Edited by Park, R. G. & Tarney, J.) Univ. of Keele, 95–104.
- Grocott, J. 1977. The relationship between Precambrian shear belts and modern fault systems. *J. geol. Soc. Lond.* 133, 257–261.
- Guchereau, J. Y. 1975. Le Saint-Barthélemy métamorphique: pétrographie et structure. Unpublished Ph. D. thesis, Toulouse.
- Kerrick, R., Allison, I., Barnett, R. L., Moss, S. & Starkey, J. 1980. Microstructural and chemical transformations accompanying deformation of granite in a shear zone at Miéville, Switzerland; with implications for stress corrosion cracking and superplastic flow. *Contr. Miner. Petrol.* 73, 221–243.
- Masch, L. 1973. Untersuchung der Aufschmelzung und Deformation der Pseudotachylyte der Silvretta (Österreich, Schweiz). *Neues Jb. Miner. Mh.* 11, 485–509.
- Masch, L. 1979. Deformation and fusion of two fault rocks in relation to their depth of formation: the hyalomylonite of Langtang (Himalaya) and the pseudotachylytes of the Silvretta nappe (Eastern Alps). *Proc. Conf. VIII Analysis of Actual Fault Zones in Bedrock*, 1–5 April 1979. National Earthquake Hazards Reduction Programme. (U.S.G.S., Menlo Park, California), 528–533.
- Park, R. G. 1961. The pseudotachylyte of the Gairloch District, Ross-shire, Scotland. *Am. J. Sci.* 259, 542–550.
- Passchier, C. W. 1981. The transformation of pseudotachylyte to ultramylonite in a mylonite zone (abstract). *J. Struct. Geol.* 3, 192.
- Schmid, S. M., Boland, J. N. & Paterson, M. S. 1977. Superplastic flow in finegrained limestone. *Tectonophysics* 43, 257–291.
- Sibson, R. H. 1975. Generation of pseudotachylyte by ancient seismic faulting. *Geophys. J. R. astr. Soc.* 43, 775–794.
- Sibson, R. H. 1977. Fault rocks and fault mechanisms. *J. geol. Soc. Lond.* 133, 191–213.
- Sibson, R. H. 1980. Transient discontinuities in ductile shear zones. *J. Struct. Geol.* 2, 165–174.
- Watts, M. J. & Williams, G. D. 1979. Fault rocks as indicators of progressive shear deformation in the Guingamp region, Brittany. *J. Struct. Geol.* 1, 323–332.
- White, S., Burrows, S. E., Carreras, J., Shaw, N. D. & Humphreys, F. J. 1980. On mylonites in ductile shear zones. *J. Struct. Geol.* 2, 175–187.
- Zwart, H. J. 1954. La géologie du massif du Saint-Barthélemy, Pyrénées, France. *Leid. geol. Meded.* 18, 1–288.
- Zwart, H. J. 1979. The geology of the central Pyrenees. *Leid. geol. Meded.* 50, 1–74.